Design and Modeling of a Single-Phase Linear Permanent Magnet Motor for Household Refrigerator Applications

Izzeldin Idris Abdalla, Taib Ibrahim, and Nursyarizal Mohd Nor

Department of Electrical and Electronic Engineering
Universiti Teknologi PETRONAS
31750 Tronoh, Malaysia
E-mails: izzeldin_abdalla@yahoo.com, taibib@petronas.com.my, nursyarizal_mnor@petronas.com.my

***Abstract*—In this paper, three novel designs of linear permanent magnet motors (LPMM) having moving magnets armature, are proposed for driving a direct drive linear reciprocating compressor in household refrigerator. The designs are then compared, including the configurations and static characteristics based on finite element analysis (FEA). In contrast to a conventional reciprocating compressor, a direct-drive linear compressor in which the piston is driven directly by a linear motor (LM) and resonant springs is considered a positive displacement. The analysis on performance of LPMM using the proposed designs is carried out on the magnetic flux-lines, magnetic field intensity, magnetic flux density, back-EMF and thrust force. The extensive simulation results indicate the effectiveness of the proposed designs.**

Keywords- *Finite Element Analysis; Linear Motor; refrigerator; quasi-Halbach; reciprocating compressor.*

I. INTRODUCTION

Nowadays, energy technologies have a crucial role in social and economic construction at all scales, from household and community to regional, national, as well as international sectors. Among its welfare effects, energy is closely linked to economic development, and grade of living. This will has further pressure on energy supplies and necessitate energy conservation measures. Meanwhile, the impact of carbon and carbon dioxide (CO_2) emission from the Kyoto protocol has increased the major concern of the researchers [1]-[7].

Of various loads, refrigeration devices represent significant and growing electrical loads, more than 14 % of the total energy consumption [8].

Undoubtedly, the household refrigerator represents one of the most important refrigerator devices in our lives today. Nevertheless, a refrigerator comprises chlorofluorocarbons (CFCs) in their installation foam which contributes to the global warming and ozone layer depletion, also the refrigerator load has a very significant impact on the emission of carbon and CO_2.

Furthermore, the electrical energy consumption of individual household refrigerator is small, however, their large number represents an appreciable potential for energy savings. These problems come due to inefficient of refrigerator compressor system [9]-[13].

Besides, one of the important issues facing the current refrigerator using a conventional compressor is that the mechanical friction of the crank-drive piston movement which is uses the concept of rotary motor. This friction lowers the performance of the refrigerator. Also, the side force between the piston and cylinder is high, thus lowering the smoothness of operation system. Fig. 1 shows schematic representation of a conventional refrigerator compressor. The compressor involves a rotary single-phase induction motor, the motor drives a reciprocating pump through a crank. The overall efficiency is relatively low, due to the inherently low efficient induction motor and the mechanical friction of the crank-driven piston movement [14]-[16].

In order to improve the performance of the conventional compressor, it must eliminate the rotary-to-linear motion conversion crank. This can reduce the volume and complexity and remove the side force on the cylinder wall caused by the crank shaft. This results in reducing the cost and power loss as well as enables soft operation system. Fig. 2 shows the schematic representation of a direct drive linear reciprocating compressor, which can satisfy the

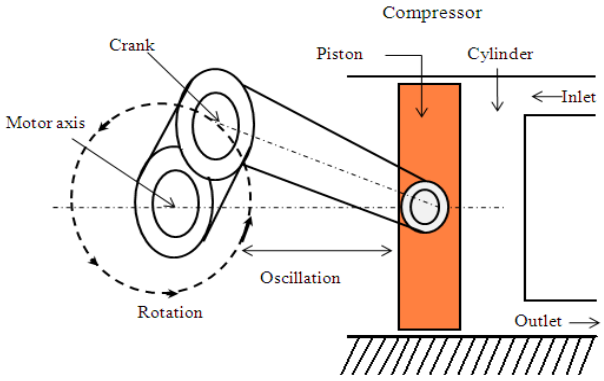

Fig. 1. Conventional refrigerator compressor [17].

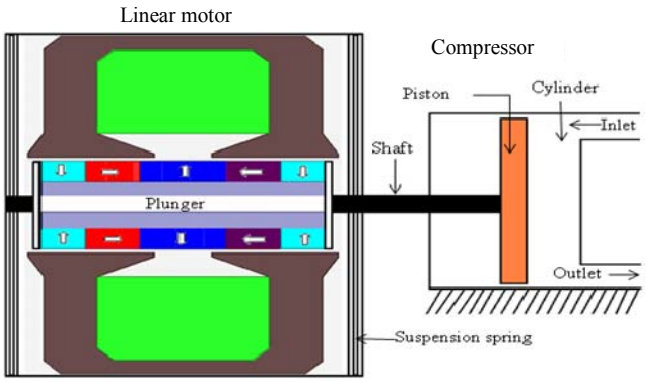

Fig. 2. Direct-drive linear compressor system [18].

aforementioned objectives, and can also operate without lubrication. In such compressor, the piston is driven by a LM and resonant springs [16], [19]. The role of spring on the system is just to store or release the energy but does not consume net energy over a cycle. The design of the LM will have an important influence on the operation of a direct-drive reciprocating compressor.

II. PREVIOUS DESIGNS

The vapor compressor designs have been proposed so far for the household refrigerator applications only presented in a few papers.

The alternative winding configurations of a short-stroke, single-phase tubular PM excited motor with quasi-Halbach magnetized armature and slotted stator with single coil for direct compressor applications was proposed by J. Wang, et. al. [20]. It has been shown that the motor design with a single stator coil has a higher thrust force capability c the three-slot, distributed winding motor design. Besides, it has high specific force per moving mass capability and high efficiency, its relative simplicity, and the availability of magnetic composite materials and high-energy rare-earth permanent magnets. These features are yield low manufacturing cost for the cost-sensitive applications [20].

As reported the linear compressor system reaches its maximum stroke and maximum input and output powers at its resonant frequency at given amplitude of the motor current, Z. Lin, et. al. [18] was proposed resonant frequency tracking technique for a high efficiency operation of a linear compressor system. By evaluating the input power to the compressor and implementing a perturb and observe algorithm, the proposed technique can adjust the frequency of the motor current to match the resonant frequency of the compressor operation. The proposed technique does not require a position sensor, and can be easily implemented in a digital controller [18].

A tubular, PMM topology which employs a 2-pole quasi-Halbach magnetized armature, having radially magnetized ring magnets placed at the centre and both ends, and a soft magnetic composite (SMC) stator core which carries a single-phase coil was proposed in [14] for linear compressor applications. Such a coil is easy to manufacture and results in a very high packing factor, which is conducive to high efficiency. All the previous designs only used the quasi-Halbach magnetized with square PMs array.

It should be noted that the foregoing treatment of the magnetization and PMs array makes it possible to improve the magnetic field distribution of the short-stroke LPMM.

III. PROPOSED DESIGN

The selection of the appropriate design was based on numerous criteria; such are force capability and simplicity. As reported, the specific force capability of LPMM may be enhanced significantly by employing a slotted stator [8], [21]. Furthermore, C-core LM requires significantly smaller volume of PM and has a largest back electromotive force (back-EMF) and force density due to the largest slot area [22], [23], thus in this paper C-core stator was selected. The airgap field of a LM can be enhanced by varying the PM shape and using the supporting tube. Furthermore, the desired flux density waveform strongly depends on the LM topology, as introduced in [5], [24], [25]. Then the three LPMM designs were proposed for vapor reciprocating compressor. These designs with different magnet shape, viz, rectangular PM (Rec_PM), trapezoidal PM (Trap_PM) and T-shape PM (TS_PM) magnet arrays with quasi-Halbach magnetization, as demonstrated in Fig. 3a, 3b and 3c, respectively. The first proposed design despite easy to design, may produce less airgap field. The second proposed design may produce more airgap field than Rec_PM; nevertheless the design of PM is more difficult than Rec_PM. The third proposed design may generate better airgap field than the two previous designs but it is facing the design complexity of PM shape. The common features of the three proposed designs are, no field winding requiring, as this will give a high thrust force capability, good dynamic performance and high efficiency.

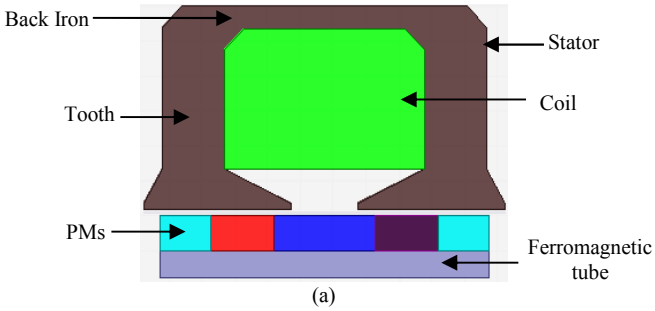

(a)

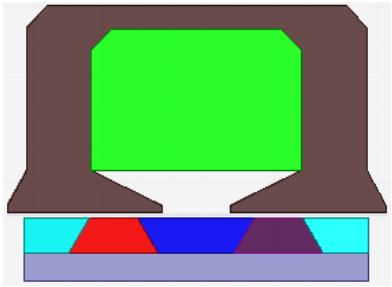

(b)

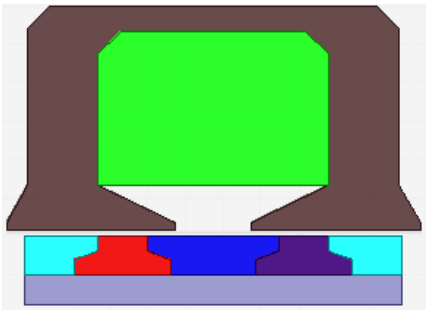

(c)

Fig. 3. 2-D FE models of a three proposed designs. (a) Geometry of Rec_PM (b) geometry of Trap_PM (c) geometry of TS_PM.

IV. Results Analysis and Discussions

Finite element analysis (FEA) software has been used to analyze the performance of the proposed designs of LPMM; such are Rec_PM, Trap_PM and TS_PM magnet array. Hence, the transient solver of this software is used to examine the electromagnetic characteristics of the three proposed designs discussed in this paper and shown in Fig. 3. Hence all results are established in cylindrical coordinate system. The main design specification parameters are tabulated in Table I.

TABLE I
DESIGN PARAMETERS OF LPMM

Description	Value
Outer radius of stator core, R_e	50.0 mm
Yoke thickness, h_{ys}	3.3 mm
Outer radius of magnet, R_m	20.0 mm
Magnet height, h_m	5.0 mm
Airgap length, g	0.8 mm
Tooth width, T_w	9.4 mm
Slot opening width, b_o	10.0 mm
Tooth tip height, h_t	1.0 mm
Magnet remanence, B_{rem}	1.14 T

The Fig. 4 show the finite element calculated open circuit flux distributions in the three proposed designs, at zero armature displacement (z_d = *0* mm). As seen at the initial position, the magnetic field distribution is highly uniform and balance and the flux produced by the permanent magnets is virtually "short-circuited" by the tooth tips. Consequently, the net flux-linkage with the coil is zero, and the flux density in the tooth body and back-iron (yoke) is also zero. The flux density waveform in the tooth tip region, both the radial and axial flux density waveforms can be approximated as trapezoidal. The peak flux entering the tooth tip occurs when the armature displacement is zero, as shown in Fig. 4.

In a similar manner, the finite element calculated open circuit flux distributions in the three proposed designs at maximum armature displacement (z_d = *11* mm) is shown in Fig. 5. At the maximum stroke position, most of the flux from the permanent magnets flows through the teeth and back-iron, and the flux-linkage with the coil is at maximum.

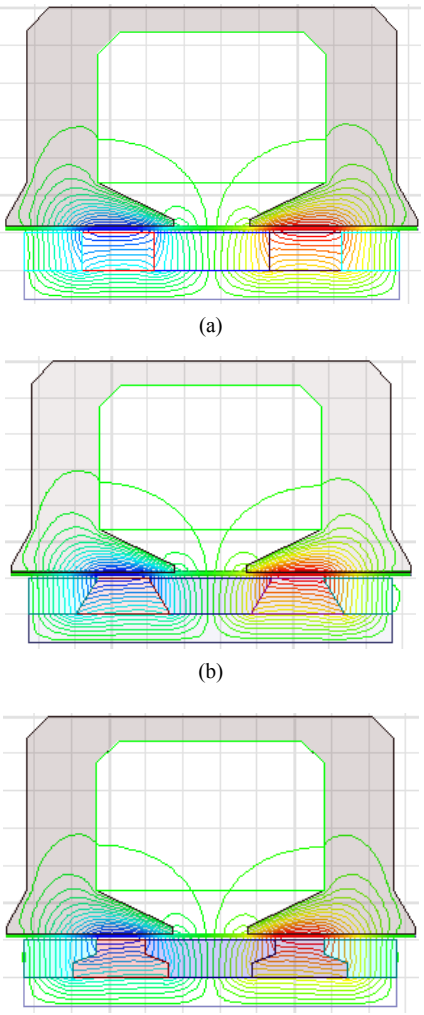

(a)

(b)

(c)

Fig. 4. 2-D FE open-circuit magnetic flux distribution in the three proposed designs of LPMM at z_d=*0* (a) flux-lines of Rec_PM (b) flux-lines of Trap_PM (c) flux-lines of TS_PM.

The flux is dominantly in radial direction. The resulting flux density in the tooth region varies with time as the armature reciprocates. The flux passing through the yoke is the same as in the tooth. However, the resulting flux density component in the yoke region is essentially in the axial direction.

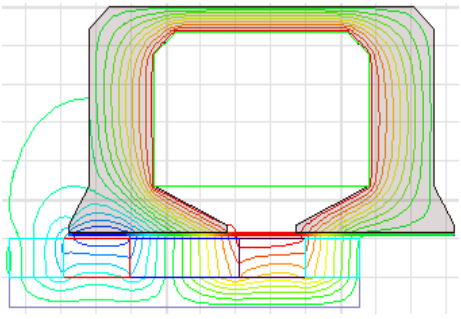

(a)

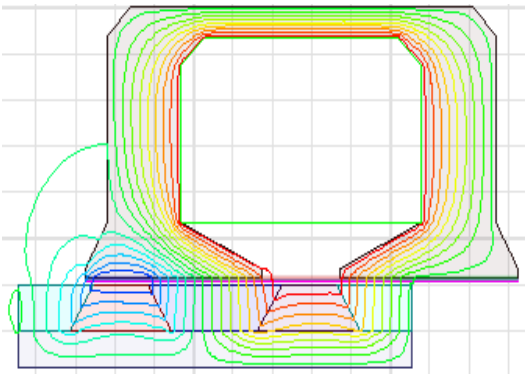

(b)

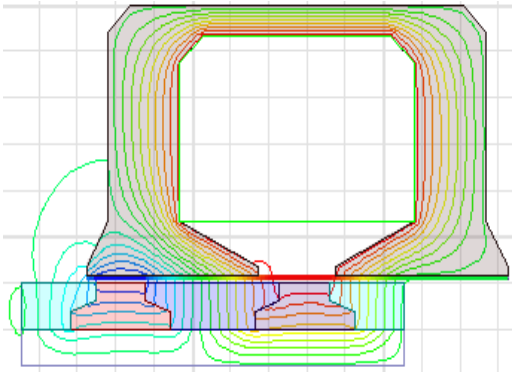

(c)

Fig. 5. 2-D FE open-circuit magnetic flux distribution in the three proposed designs of LPMM at z_d=*11* mm (a) flux-lines of Rec_PM (b) flux-lines of Trap_PM (c) flux-lines of TS_PM.

In order to compare the performances of the three proposed designs given in section III, the simulation results of the open- circuit magnetic field were established.

Fig. 6 shows comparison among magnetic flux-lines distribution at the airgap of the three proposed designs, such are rectangular, trapezoid and T-shape magnet array. All the results are showed at z_d =*0*. Simulation results reveal that the higher flux lines obtained for Rec_PM shape magnet array, line with solid triangles, the second higher flux line is showed for trapezoid magnet array, line with solid circles and the line with solid boxes showed for the rectangular magnet array. From Fig. 6, the maximum fluxes are, 0.0842 mwb/m, 0.0806 mwb/m and 0.0773 mwb/m for the proposed designs, Rec_PM, Trap_PM and TS_PM magnet array, respectively, while the average values are, 0.0026μwb/m, 0.0062 μwb/m and 0.0054 μwb/m. This makes actuating force of the LM with Trap_PM magnet array larger than the other two proposed designs. It can be seen that the waveform is very close to sinusoidal, subsequently, the back EMF can be determined by the waveform of the flux, which approximately sinusoidal, Eq (1) shows the back-EMF calculation method by using flux.

$$E = \sqrt{2}\pi f N_c k_N \phi \qquad (1)$$

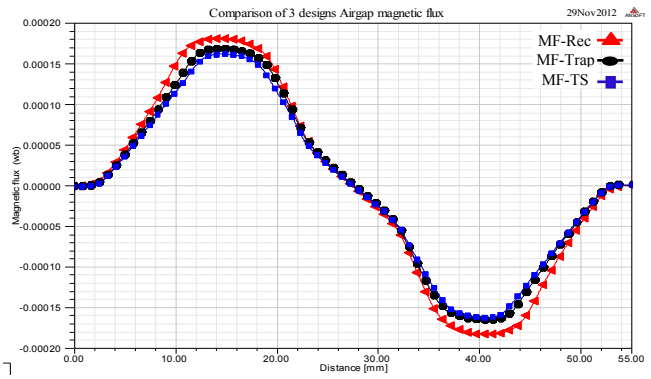

Fig. 6. Comparison between the simulation results of magnetic flux lines distribution at the airgap of the proposed designs.

where f in Hz is the operating frequency, N_c is the number of turns of coil, and k_N is the winding factor, which equals 1[26], [27].

The simulation results of magnetic field intensity (H) at airgap at z_d =*0* were established for the three proposed designs and compared as in Fig. 7. From the results, it is found that the higher amplitude of airgap magnetic field intensity obtained for the proposed design Rec_PM, line with solid triangles. Second higher amplitude showed for the proposed design Trap_PM, line with solid circles and the line with boxes showed for the third.

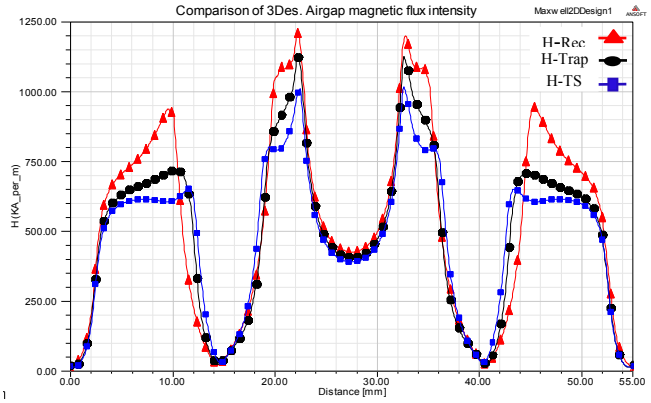

Fig. 7. Comparison between the simulation results of the magnetic field intensity at airgap of the proposed designs.

Fig. 8 shows a comparison among the simulation results of the magnetic flux density (B) at airgap of the three proposed designs at z_d = *0*. It is found that the amplitudes of airgap flux density of motors as follow the higher amplitude obtained for the proposed design Rec_PM, line with solid triangles. Second higher amplitude showed for the proposed design Trap_PM, line with solid circles and the line with boxes showed for the proposed design TS_PM. Meanwhile, the average value of the magnetic flux density is found to be 0.507634 T for the proposed design Rec_PM, 0.523129 T for the proposed design Trap_PM and 0.518091 T for the proposed design TS_PM. The relationship between magnetic field intensity and magnetic flux density is expressed as in Eq (2) [28].

$$B = \mu_0 H \quad (2)$$

where μ_0 is the permeability of free space $= 4\pi * 10^{-7}\ H/m$.

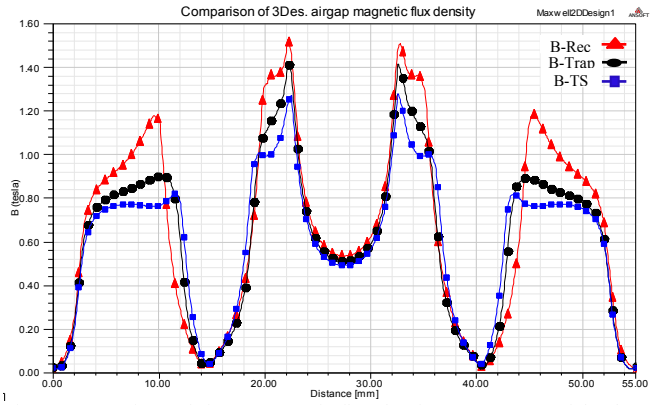

Fig. 8. Comparison of airgap magnetic flux density components of the three proposed designs.

When the mover is moving along the z-direction, so the magnetic field while the stator is static; hence, the distribution of the air gap magnetic field varies with the position of mover. So, the flux coupled with winding is varied with time. The back *EMF* can be written as in Eq (3)

$$E = \frac{d\psi}{dt} = \frac{d\psi}{dz} * \frac{dz}{dt} = v * \frac{d\psi}{dz} \quad (3)$$

where v is the motor velocity along the z-direction. Thus, back EMF is given by the product of velocity v and the rate of change in flux linkage (ψ), with respect to position.

Based on finite element (FE) analysis, the open-circuit flux-linkage and back-EMF waveforms of the three designs are compared in Fig. 9 and Fig. 10, respectively. The average value of the back EMF was found to be, 228.128 V, 233.4009 V and 232.8276 V for Rec_PM, Trap_PM and TS_PM, respectively. Obviously, the flux-linkages and back-EMF of the T-shape magnet array and trapezoidal magnet arrays are superior over the rectangular magnet array design.

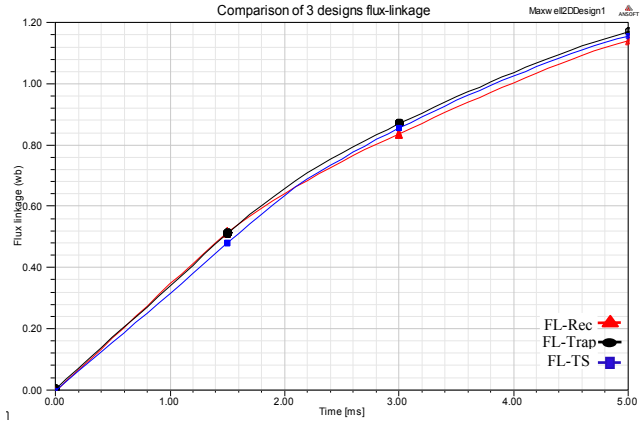

Fig. 9. Comparison of flux-linkage of the three proposed designs.

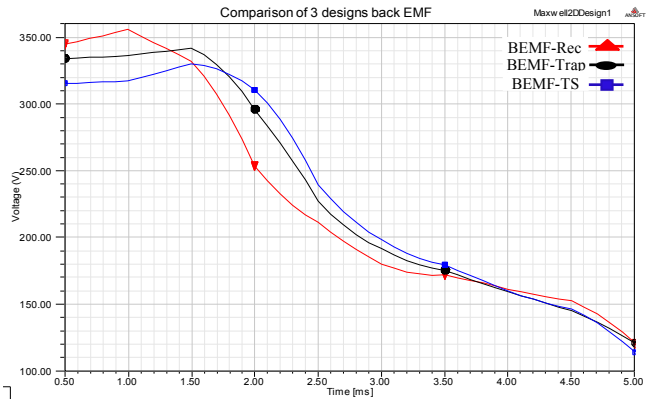

Fig. 10. Comparison of back EMF of the three proposed designs.

Fig. 11 compares the FE-predicted thrust force of the three proposed designs for an excitation current of 0.5 A. The average thrust forces are quantified as 51.81488 N, 45.43742 N and 40.04353 N for the Rec_PM, Trap_PM and TS_PM, respectively.

Fig. 11. Comparison of the thrust force of the three proposed designs

V. Conclusion

This paper has proposed three novel designs of moving-magnet LPMM for vapor reciprocating compressor in a household refrigerator. The proposed designs have different magnet shapes; viz, rectangular (Rec_PM), trapezoidal (Trap_PM) and T-shape (TS_PM) magnet array with quasi-Halbach magnetization. A Maxwell 2-D model was developed for each one and the results have been established which ensured efficient operation of LPMM. The simulation results reveal that the moving-magnet LPMM with T-shape magnet array and trapezoidal magnet arrays are superior over the rectangular magnet array design, in terms of flux linkage, Back EMF and cogging force. Subsequently, the analysis of motor performance reveals that the flux density increases with the increase of magnet width.

Acknowledgment

The authors would like to thank University Teknologi PETRONAS (UTP), 3170 Tronoh, Perak, Malaysia for the financial support.

REFERENCES

[1] B. W. Ang and G. Pandiyan, "Decomposition of energy-induced CO2 emissions in manufacturing," *Energy Economics*, vol. 19, no. 3, pp. 363-374, Jul. 1997.

[2] M. F. Henriques, F. Dantas, and R. Schaeffer, "Potential for reduction of CO2 emissions and a low-carbon scenario for the Brazilian industrial sector," *Energy Policy*, vol. 38, no. 4, pp. 1946-1961, Apr. 2010.

[3] R. Ramanathan, "A multi-factor efficiency perspective to the relationships among world GDP, energy consumption and carbon dioxide emissions," *Technological Forecasting and Social Change*, vol. 73, no. 5, pp. 483-494, Jun. 2006.

[4] S. J. Lin, I. J. Lu, and C. Lewis, "Identifying key factors and strategies for reducing industrial CO2 emissions from a non-Kyoto protocol member's (Taiwan) perspective," *Energy Policy*, vol. 34, no. 13, pp. 1499-1507, Sep. 2006.

[5] B. Janet Ruiz-Mendoza and C. Sheinbaum-Pardo, "Electricity sector reforms in four Latin-American countries and their impact on carbon dioxide emissions and renewable energy," *Energy Policy*, vol. 38, no. 11, pp. 6755-6766, Nov. 2010.

[6] W.-qiang Sun, J.-ju Cai, H.-jun Mao, and D.-jiao Guan, "Change in Carbon Dioxide (CO2) emissions from energy use in china's iron and steel industry," *Journal of Iron and Steel Research, International*, vol. 18, no. 6, pp. 31-36, Jun. 2011.

[7] H. Dai, T. Masui, Y. Matsuoka, and S. Fujimori, "The impacts of China's household consumption expenditure patterns on energy demand and carbon emissions towards 2050," *Energy Policy*, vol. 50, pp. 736-750, Nov. 2012.

[8] J. Wang, D. Howe, and Z. Lin, "Comparative studies on linear motor topologies for reciprocating vapor compressors," in *IEEE International Electric Machines & Drives Conference, 2007. IEMDC '07.*, 2007, vol. 2, no. c, pp. 364-369.

[9] P. Binneberg, E. Kraus, and H. Quack, "Reduction in power consumption of household refrigerators by using variable speed compressors," in *International refrigeration and air conditioning conference*, 2002.

[10] M. L. M. Stoop and A. J. D. Lambert, "Processing of discarded refrigerators in the Netherlands," *Technovation*, vol. 18, no. 2, pp. 101-110, Feb. 1998.

[11] S. Wongwises and N. Chimres, "Experimental study of hydrocarbon mixtures to replace HFC-134a in a domestic refrigerator," *Energy Conversion and Management*, vol. 46, no. 1, pp. 85-100, Jan. 2005.

[12] J. M. Calm and D. A. Didion, "Trade-offs in refrigerant selections□: past , present , and future," *lntJ. Refrig.*, vol. 21, no. 4, pp. 308-321, 1998.

[13] S. Hou, H. Li, and H. Zhang, "An open air–vapor compression refrigeration system for air-conditioning and desalination on ship," *Desalination*, vol. 222, no. 1–3, pp. 646-655, Mar. 2008.

[14] J. Wang, D. Howe, and Z. Lin, "Design optimization of short-stroke single-phase tubular permanent-magnet motor for refrigeration applications," *IEEE Transactions on Industrial electronics*, vol. 57, no. 1, pp. 327-334, 2010.

[15] J. Wang, Z. Lin, and D. Howe, "Analysis of a short-stroke , single-phase , quasi-Halbach magnetised tubular permanent magnet motor for linear compressor applications," *Electric Power Applications, IET*, vol. 2, no. 3, pp. 193-200, 2008.

[16] J. Wang, T. Ibrahim, and D. Howe, "Prediction and measurement of iron loss in a short-stroke , single phase , tubular permanent magnet machine," *IEEE Transactions on Magnetics*, vol. 46, no. 6, pp. 1315-1318, 2010.

[17] I. Boldea and S.A. Nasar, "Linear electric actuators and generators," *IEEE Transactions on Energy Conversion*, vol. 14, no. 3, pp. 712-717, 1999.

[18] T. Ibrahim, "Short-stroke, single-phase tubular permanent magnet motors for refrigeration applications," University of Sheffield, Department of Electronic and Electrical Engineering, 2009.

[19] Y. Amara, J. Wang, and D. Howe, "Analytical prediction of eddy-current loss in modular tubular permanent-magnet machines," *IEEE Trans. Energ. Conver.*, vol. 20, no. 4, pp. 761-770, 2005.

[20] Z. Lin, J. Wang, and D. Howe, "A resonant frequency tracking technique for linear vapor compressors," in *Electric Machines & Drives Conference*, 2007, pp. 370-375.

[21] J. Wang, D. Howe, and Z. Lin, "Comparative study of winding configurations of short-stroke , single phase tubular permanent magnet motor for refrigeration applications," in *Industry Applications Conference, 2007. 42nd IAS Annual Meeting. Conference Record of the 2007 IEEE*, 2007, pp. 311-318.

[22] H. Lu, J. Zhu, Z. Lin, and Y. Guo, "A miniature short stroke linear actuator — design and analysis," *IEEE Transactions on Magnetics*, vol. 44, no. 4, pp. 497-504, 2008.

[23] Q. Lu, M. Yu, Y. Ye, Y. Fang, and J. Zhu, "Thrust force of novel PM transverse flux linear oscillating actuators with moving magnet," *IEEE Transactions on Magnetics*, vol. 47, no. 10, pp. 4211-4214, 2011.

[24] W. Min, J. T. Chen, Z. Q. Zhu, Y. Zhu, M. Zhang, and G. H. Duan, "Optimization and comparison of novel E-core and C-core linear switched flux PM machines," *IEEE Transactions on Magnetics*, vol. 47, no. 8, pp. 2134-2141, 2011.

[25] J. Lee, E. M. Dede, and T. Nomura, "Simultaneous design optimization of permanent magnet , coils , and ferromagnetic material in actuators," *IEEE Transactions on Magnetics*, vol. 47, no. 12, pp. 4712-4716, 2011.

[26] H.-hao Luo, J. Wu, and W.-sen Chang, "Minimizing thrust fluctuation in moving-magnet permanent-magnet brushless linear DC motors," *IEEE Transactions on Magnetics*, vol. 43, no. 5, pp. 1968-1972, 2007.

[27] Y. Guo, J. X. Jin, J. G. Zhu, and H. Y. Lu, "Design and analysis of a prototype linear motor driving system for HTS maglev transportation," *IEEE Trans. Applied Superconductivity*, vol. 17, no. 2, pp. 2087-2090, 2007.

[28] J. R. Brauer, *Magnetic Actuators and Sensors*. John Wiley & Sons, Inc., Hoboken, New Jersey and Canada, 2006, pp. 12-13.